TELKOMNIKA, Vol. 11, No. 5, May 2013, pp. 2753 ~ 2762
ISSN: 2302-4046

A DC Error Self-Correcting Circuit for the Capacitive Micromachined Gyroscope

Bing Mo[1]*, Jun Cai[2], Chaodong Ling[3]
[1,3]Department of Electrical Engineering, Huaqiao University, Xiamen 361021, China
[2]Department of electronics and information engineering, Communication University of China, Beijing 100024, China
*Corresponding author, e-mail:mobing@hqu.edu.cn

Abstract

Micromachined gyroscope always contains two groups of capacitors, one is the driving capacitor, which is used to drive the micromachined gyroscope, to make sure the gyroscope could oscillate along the driving direction. The other is so called the sensing capacitor, which used to detect the displacement along the sensing direction, in order to detect the input angle velocity. Since there are some imperfections during the machining process, the static value of the driving capacitor and sensing capacitor always have some variations. These variations would cause some bad effects in the integrated circuit. In this paper, the variations of driving capacitor and sensing capacitor are analyzed based on the principle of integrated circuit. It is shown that the effect caused by driving capacitor variation would be cancelled in the signal processing, but the driving capacitor variation could cause a DC error signal at the output node of the first LPF in the integrated circuit. This DC error would distort the desired signal at the output node of the amplitude amplifier. So that a DC error self-correcting circuit is designed, both the simulation results and the testing results show that DC error could be self-corrected by this additional circuit.

Keywords*: micromachined gyroscope; capacitor variation; DC error; self-correcting circuit*

1. Introduction

Micromachined gyroscope is the key research field because it is widely applied in both civil and military field [1-5]. Owing to the characters of simple structure, high sensitivity and low temperature drift, capacitive micromachined gyroscope becomes one of the most popular gyroscopes [6-9]. However, the static value of the capacitor has a deviation because of the imperfections during the machining process [10-13]. The deviation would deteriorate the desired signal in integrated circuit. Based on the principle of integrated circuit, the effect of capacitive deviation is analyzed in this paper. The result shows that the deviation of driving capacitor could be cancelled during the signal processing in the integrated circuit. But the deviation of sensing capacitor induces a DC error at the output node of the first LPF in integrated circuit. This DC error would distort the desired signal at the output node of the amplitude amplifier, which also decreases the output range of the sensor system. In order to cancel this DC error, a DC error self-correcting circuit is designed. Both the simulation and testing result are presented to prove it works properly.

2. Principle of Capacitive Micromachined Gyroscope

2.1. Structure of a Capacitive Micromachined Gyroscope

Figure 1 shows the structure of a capacitive micromachined gyroscope. It is an inside sensing outside driving frame micromachined gyroscope. There are two movable directions as shown in Figure 1, one is the driving direction (marked as X direction in Figure 1), the other is the sensing direction (marked as Y direction). The gyroscope contains two masses: outer mass and inner mass. Outer mass is connected to anchors by driving springs, and sensing springs connect inner mass to outer mass. If outer mass is forced by a sine electrostatic driving force, it may oscillate along the X direction, inner mass would also oscillate along the X direction because it is connected to outer mass by sensing springs. At the same time, if there is an input angle velocity in the Z direction, Coriolis force generates by Coriolis effect, and inner mass

Received January 5, 2013; Revised March 19, 2013; Accepted March 27, 2013

moves along the Y direction because the direction of Coriolis force is along the Y direction. So that, inner mass has a displacement along the Y direction, which induces a variation of equivalent capacitor of sensing combs. The displacement of inner mass along the Y direction is linear to the input angle velocity, to detect the variation of sensing capacitor, we could calculate the input angle velocity. This is the fundamental of capacitive micromachined gyroscope.

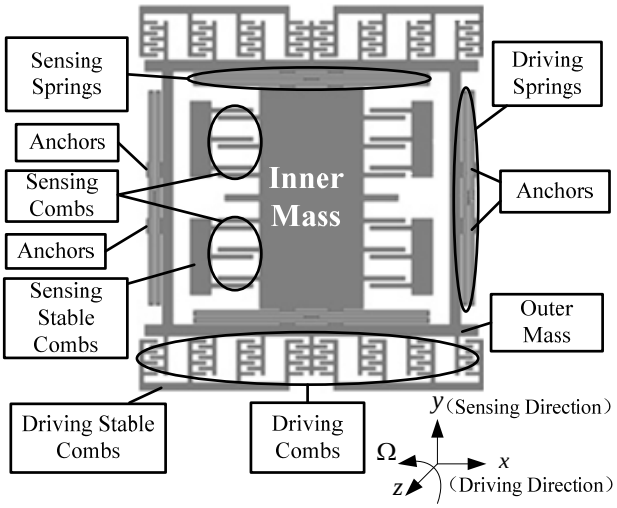

Figure 1. Structure of capacitive micromachined gyroscope

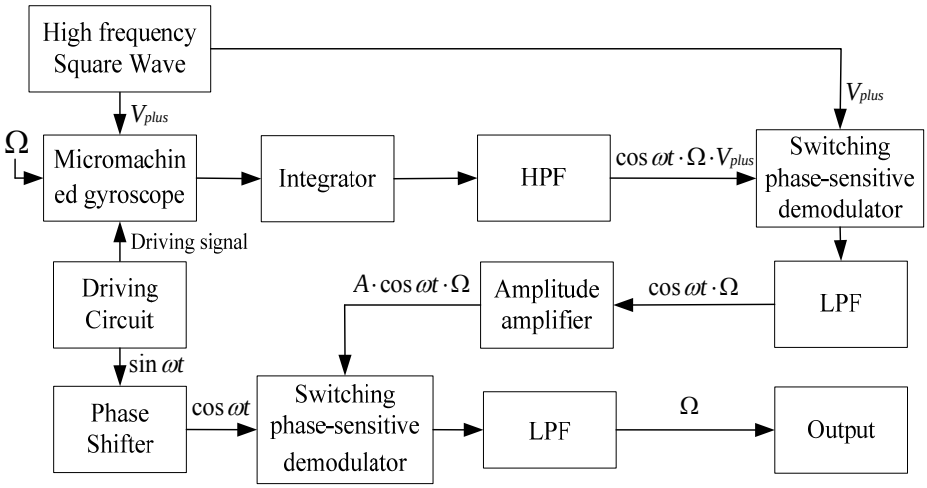

Figure 2. Structure of capacitive micromachined gyroscope

2.2. Principle of Integrated Circuit for Capacitive Micromachined Gyroscope

Since the variation of sensing capacitor caused by Coriolis force is rather small, almost at atto farad (10^{-18}F) level. So that the desired signal is always modulated to high frequency in order to reduce the 1/f noise. Then by demodulation, the desired signal is detected at the output node.

The principle of sensing circuit is showed in Figure 2, which contains a modulation and two demodulation process. The variation of sensing capacitor signal is modulated by the high frequency square wave as shown in Figure 2. Integrator is used to achieve modulation and the capacitance to voltage transformation. HPF could filter both the low frequency 1/f noise and the coupling driving signal. After two demodulation process, the input angle velocity Ω can be

detected at the output node in the form of voltage or current. The amplitude amplifier circuit in Figure 2 is used to increase the sensitivity of the micromachined gyroscope.

2.3. Integrator

As discussed before, integrator not only achieves the modulation function, but also transforms the capacitance to voltage. The principle of integrator is presented in Figure 3, where op-amp means an operational amplifier, C3 is the integrating capacitor, C1 and C2 are the equivalent capacitor of sensing combs.

Suppose C1-C2=2ΔC, where ΔC represents the variation of sensing capacitor of micromachined gyroscope. The fixed plates of C1 and C2 are applied the high frequency modulation signal V_{plus} and $-V_{plus}$ respectively. The current i_1、i_2 and i in Figure 3 can be expressed as the following equations.

$$i_1 = V_{plus} \cdot j\omega C_1 \tag{1}$$

$$i_2 = -V_{plus} \cdot j\omega C_2 \tag{2}$$

$$i = i_1 + i_2 = j\omega (C_1 - C_2) \cdot V_{plus} = 2 j\omega \Delta C \cdot V_{plus} \tag{3}$$

Since the total current i passes through the integrating capacitor C3, the output voltage of the integrator can be expressed as:

$$V_{o-int} = -i \times \frac{1}{j\omega C_3} = -\frac{2\Delta C}{C_3} \cdot V_{plus} \tag{4}$$

From equation (4), $V_{o\text{-}int}$ is proportional to $\Delta C \cdot V_{plus}$. It proves that integrator not only achieves the modulation function, but also transforms the capacitance to voltage.

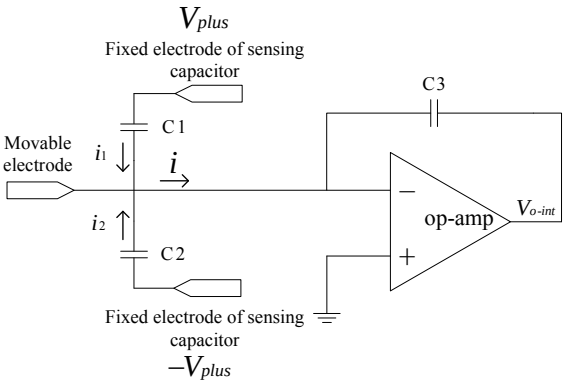

Figure 3. Principle of integrator

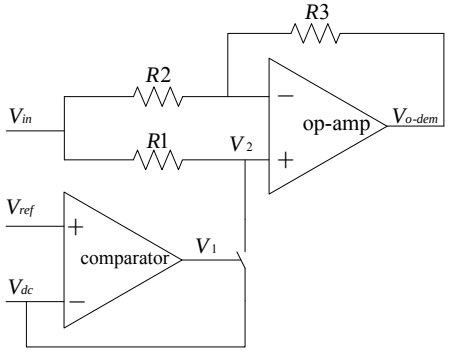

Figure 4. Switching phase-sensitive demodulator

2.4. Switching Phase-Sensitive Demodulator

Switching phase-sensitive demodulator is used to carry out signal demodulate, the detail of this circuit is shown in Figure 4. The demodulator includes a comparator, a switch and an operational amplifier, and in Figure 4, the values of R1、R2、R3 are equal.

The signal V_{ref} has the equivalent frequency and phase with the envelope signal of input signal V_{in}, suppose the signal at the output node of comparator is V_1. So that V_1 is a square wave signal with exactly same frequency and phase as the envelope signal of input signal V_{in}. Switch connects the positive input node of operational amplifier to reference voltage V_{dc}, which is a DC balanced voltage. The switch is controlled by signal V_1, so that the signal V_2 is:

$$V_2 = \begin{cases} 0 & nT_C < t < \left(n+\frac{1}{2}\right)T_C \\ V_{in} & \left(n+\frac{1}{2}\right)T_C < t < (n+1)T_C \end{cases} \quad (5)$$

Where, T_c is the period of signal Vref.

Because of the values of R1、R2、R3 are equal, the signal at output node can be expressed as:

$$V_{o-dem} = -V_{in} + 2V_2 \quad (6)$$

Substituting equation (5) into equation (6), we can easily get the following equation

$$V_{o-dem} = \begin{cases} -V_{in} & nT_C < t < \left(n+\frac{1}{2}\right)T_C \\ V_{in} & \left(n+\frac{1}{2}\right)T_C < t < (n+1)T_C \end{cases} \quad (7)$$

We can replace equation (7) as equation (8) and equation (9)

$$V_{o-dem} = V_{in} \cdot K \quad (8)$$

$$K = \begin{cases} -1 & nT_C < t < \left(n+\frac{1}{2}\right)T_C \\ +1 & \left(n+\frac{1}{2}\right)T_C < t < (n+1)T_C \end{cases} \quad (9)$$

In Figure 2, there are two demodulation processes. The input signal of first demodulation can be expressed as:

$$U_s(t) = \mathrm{K}_1 \cdot \Omega \cdot \cos \omega t \cdot V_{plus} \quad (10)$$

Where, K_1 is a constant, it is proportional to the amplifier coefficient before the first demodulation. Ω is the input angle velocity, cosωt is the displacement of movable plate along the sensing direction. V_{plus} is the high frequency modulation signal, suppose the frequency and amplitude of V_{plus} are ω_1 and V_{amp} respectively. The Fourier expansion of V_{plus} is:

$$V_{plus} = \frac{4}{\pi}\mathrm{V}_{amp}\left(\sin \omega_1 t + \frac{1}{3}\sin 3\omega_1 t + \frac{1}{5}\sin 5\omega_1 t + \cdots\right) \quad (11)$$

The reference signal of the first demodulation in the integrated circuit is V_{plus}, so that equation (9) can be expressed as:

$$K = -\frac{4}{\pi}\left(\sin \omega_1 t + \frac{1}{3}\sin 3\omega_1 t + \frac{1}{5}\sin 5\omega_1 t + \cdots\right) \quad (12)$$

Substituting equation (10) (11) and (12) into equation (8), and using the product to sum formula, we could get:

$$
\begin{aligned}
&U_o(t) = \mathrm{K}_1 \cdot \Omega \cdot \cos \omega t \cdot V_{plus} \cdot K \\
&= -\frac{16}{\pi^2} \cdot \mathrm{K}_1 \cdot \Omega \cdot \cos \omega t \cdot \mathrm{V}_{amp} \left(\sin \omega_1 t + \frac{1}{3} \sin 3\omega_1 t + \frac{1}{5} \sin 5\omega_1 t + \cdots \right)^2 \\
&= -\frac{16\mathrm{K}_1 \mathrm{V}_{amp}}{\pi^2} \cdot \Omega \cdot \cos \omega t \left(\mathrm{A} + \mathrm{B} \cos 2\omega_1 t + \mathrm{C} \cos 4\omega_1 t + \mathrm{D} \cos 6\omega_1 t + \cdots \right)
\end{aligned} \tag{13}
$$

Where, A、B、C、D are constant. A can be expressed as

$$
\mathrm{A} = \frac{1}{2}\left(1 + \frac{1}{9} + \frac{1}{25} + \frac{1}{49} + \frac{1}{81} + \cdots\right) = \frac{1}{2} \cdot \frac{\pi^2}{8} = \frac{\pi^2}{16} \tag{14}
$$

Substituting equation (14) into equation (13), we could get:

$$
U_o(t) = -\mathrm{K}_1 \mathrm{V}_{amp} \cdot \Omega \cdot \cos \omega t - \frac{16\mathrm{K}_1 \mathrm{V}_{amp}}{\pi^2} \cdot \Omega \cdot \cos \omega t \left(\mathrm{B} \cos 2\omega_1 t + \mathrm{C} \cos 4\omega_1 t + \mathrm{D} \cos 6\omega_1 t + \cdots \right) \tag{15}
$$

In equation (15), there is a multinomial inside the parentheses on the right side of the equal sign, every item in this multinomial a cosine function with the frequency of even times of ω_1. Since ω_1 is much bigger than the frequency of driving signal ω, the second item on the right side of the equal sign in equation (15) can be filtered by a low pass filter with the frequency higher than ω but lower than $2\omega_1$. After the low pass filter, only the signal $-K_1 \cdot V_{amp} \cdot \Omega \cdot \cos\omega t$ leaves.

The second switching phase-sensitive demodulator is exactly same as we discussed before. But the input signal is $-K_1 \cdot V_{amp} \cdot \Omega \cdot \cos\omega t$ and the reference demodulation signal is $\cos\omega t$ in this demodulator. After the two demodulation processing, the output signal is proportional to the input angle velocity Ω.

2.5. Simulation Results of Integrated Circuit.

Figure 5 shows the simulation results of the total circuit. Where V_{in} is the input angle velocity with the 50Hz frequency and 1V amplitude. V_{out1} is the signal at the integrator output node, which is an envelope signal. V_{lpf1} is the signal at first LPF output node, we could find it is already demodulated for the first time, and V_{lpf2} is the signal at second LPF output node, this signal is proportional to the input angle velocity Ω.

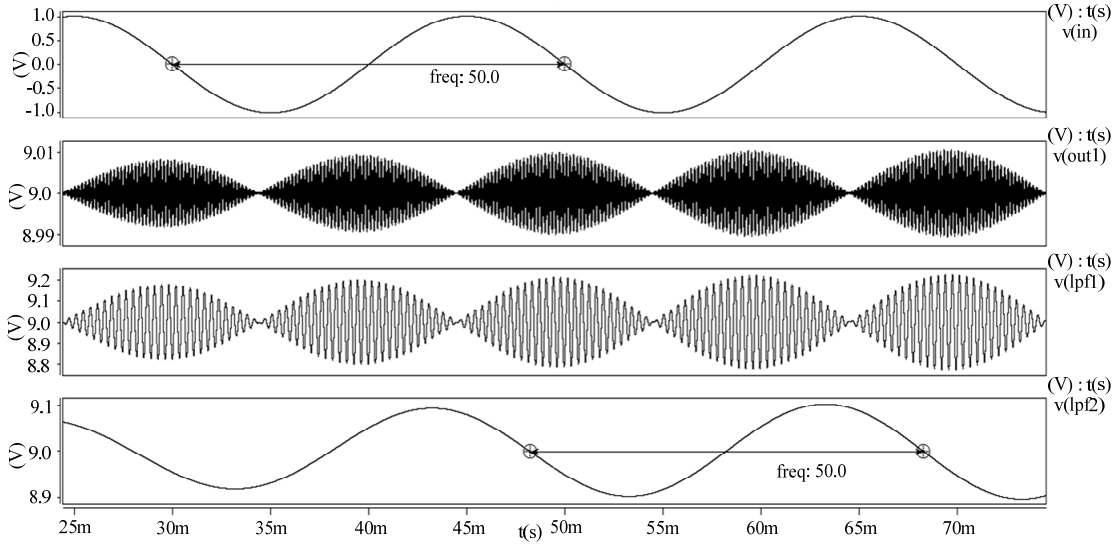

Figure 5. Simulation results of integrated circuit

3. The Effects of Driving Capacitor Deviation

The micromachined gyroscope sensor shown in Figure 1 is equivalent to two groups of capacitors, the sketch of connection between micromachined gyroscope sensor and integrated circuit is shown in Figure 6. Where C4 and C5 are the driving capacitors and C1 and C2 are the sensing capacitors. In ideal condition, the value of C4 equals to C5, and the value of C1 equals to C2. But it is hard to achieve in actual condition because of the imperfections during machining process. If there is deviation between C4 and C5, the AC signal V_{ac}·sinωt would couples to node 1 in Figure 6. Since the frequency ω is much lower than -3dB frequency of HPF which is following the integrator in Figure 2, the coupling signal V_{ac}·sinωt would be filtered and would not cause any problem in the following demodulation processing.

Figure 7 shows the comparison of simulation between ideal condition and the condition of there is deviation between C4 and C5. Suppose the deviation between C4 and C5 is 1% of their stable value, and the frequency of driving signal is 2755.4Hz. In Figure 7, out1 is the signal in the output node of integrator, in ideal condition, it is an envelope signal, but in the condition with deviation, the coupling driving signal deteriorates the desired signal. Compare the output signal at the HPF output node of two conditions, it is easy to observe that the signal of these two conditions are quite similar. It means that the coupling driving signal has been filtered by HPF.

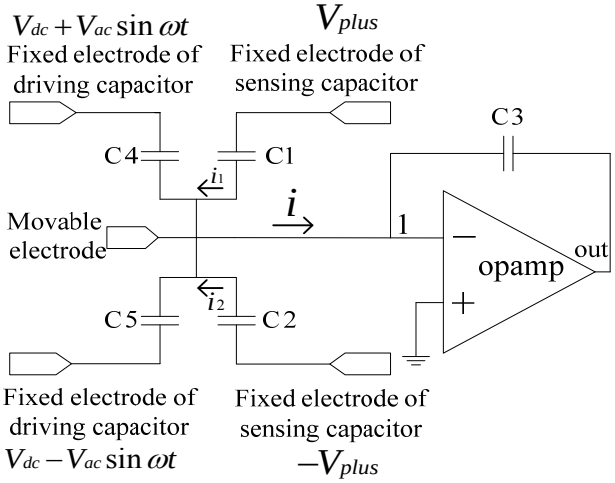

Figure 6. Sketch of connection between micromachined gyroscope sensor and ASIC

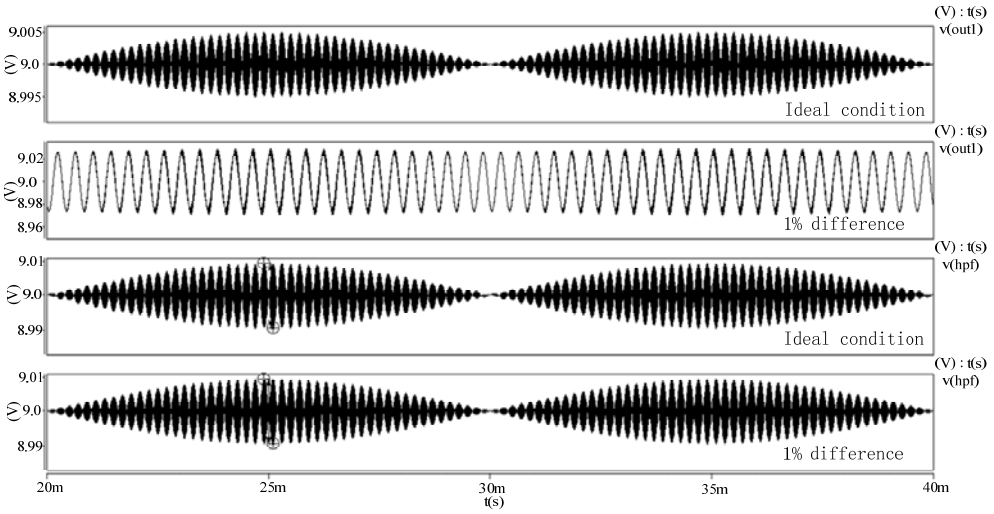

Figure 7. Comparison of ideal condition with the condition with 1% departure of driving equivalent capacitance

4. The Effects of Sensing Capacitor Deviation

In Figure 6, if there is deviation between C1 and C2, then the high frequency demodulation signal Vplus would be coupling to node 1. Suppose C1=C2+ΔCs, then the current i_1 and i_2 in Figure 6 can be expressed as equation (16) and equation (17) respectively.

$$i_1 = V_{plus} \cdot j\omega C_1 \tag{16}$$

$$i_2 = -V_{plus} \cdot j\omega C_2 \tag{17}$$

And the sum current i in Figure 6 is:

$$i = i_1 + i_2 = V_{plus} \cdot j\omega (C_1 - C_2) = V_{plus} \cdot j\omega \Delta C_s \tag{18}$$

The voltage at the output node of integrator is:

$$V_{err-s} = i \cdot \frac{1}{j\omega C_3} = V_{plus} \cdot j\omega \Delta C_s \cdot \frac{1}{j\omega C_3} = \frac{\Delta C_s}{C_3} V_{plus} \tag{19}$$

From equation (19), we could get the conclusion that if deviation between C1 and C2 is ΔCs, the coupling signal at the output node of integrator is $\Delta Cs \cdot V_{plus}$ /C3, where C3 is the integrating capacitor. Since the coupling signal is linear to V_{plus}, and the fundamental frequency of V_{plus} is higher than the -3dB frequency of HPF. So that HPF is helpless to this coupling signal. The coupling signal is also processed by the first switching phase-sensitive demodulator. In mathematics, we could multiply equation (19) to equation (12) in order to express the coupling signal processing, the result is:

$$\begin{aligned} V_{err-s} \cdot K &= \frac{\Delta C_s}{C_5} V_{plus} \cdot K = -\frac{16}{\pi^2} \frac{\Delta C_s}{C_3} V_{amp} \left(\sin \omega_1 t + \frac{1}{3} \sin 3\omega_1 t + \frac{1}{5} \sin 5\omega_1 t + \cdots \right)^2 \\ &= -\frac{16}{\pi^2} \frac{\Delta C_s}{C_5} V_{amp} \left(A + B\cos 2\omega_1 t + C\cos 4\omega_1 t + D\cos 6\omega_1 t + \cdots \right) \end{aligned} \tag{20}$$

Where, V_{amp} is the amplitude of V_{plus}, A、B、C、D are constant. It could be calculated that $A=\pi^2/16$, then:

$$\begin{aligned} V_{err-s} \cdot K &= -\frac{16}{\pi^2} \frac{\Delta C_s}{C_3} V_{amp} \left(A + B\cos 2\omega_1 t + C\cos 4\omega_1 t + D\cos 6\omega_1 t + \cdots \right) \\ &= -\frac{\Delta C_s}{C_5} V_{amp} - \frac{16}{\pi^2} \frac{\Delta C_s}{C_3} V_{amp} \left(B\cos 2\omega_1 t + C\cos 4\omega_1 t + D\cos 6\omega_1 t + \cdots \right) \end{aligned} \tag{21}$$

After the first LPF following the first switching phase-sensitive demodulator, high frequency component of the coupling signal shown in equation (12) is filtered, only the DC component of the coupling signal leaves, it can be expressed as:

$$V_{err-dc} = -\Delta C_s V_{amp} / C_3 \tag{22}$$

Normally, ΔCs is almost more than one percent of stable value of C1 because of imperfections during machining process, meanwhile, the value of ΔC in equation (4) is not more than one per mille. So that the DC coupling signal shown in equation (12) is almost more than ten times of amplitude of desired signal.

In Figure 2, the first LPF is followed by an amplitude amplifier circuit. In this case, the DC coupling signal would also be amplified. It may easy induce distortion of desired signal.

Figure 8 shows the comparison of simulation results between ideal condition and the condition of deviation between C1 and C2 is 1% of their stable value. Suppose the input angle velocity is sine signal with 50Hz frequency and 1V amplitude. We could found that the DC coupling signal at the first LPF output node is almost 2.4V. Meanwhile, the amplitude of desired

signal is 0.2238V, less than 1/10 of the value of DC coupling signal. After amplitude amplifier circuit, the distortion of desired signal can be observed easily. If the deviation between C1 and C2 or the gain of amplitude amplifier circuit increases, distortion would deteriorate, so that it is necessary to cancel the DC coupling signal V_{err-dc} at the output node of first LPF.

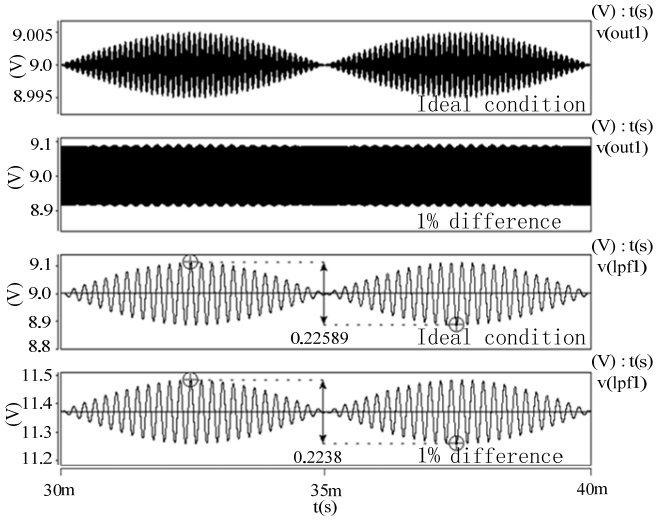

Figure 8. Comparison of ideal condition with the condition with 1% departure of sensing equivalent capacitance

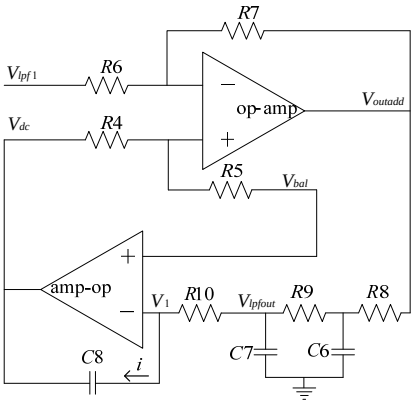

Figure 9. Sketch of DC error self-correcting circuit

5. DC Error Self-Correcting Circuit

In order to cancel the DC coupling signal V_{err-dc} at the output node of first LPF, a DC error self-correcting circuit is designed. The principle of this circuit is shown in Figure 9, where the upper operational amplifier together with the identical resistance resistors R4、R5、R6 and R7 compose an in-phase sum circuit. The lower operational amplifier and capacitor C8 compose an integrator. A two-order LPF is composed of resistors R8、R9 and capacitors C6、C7. The input node of this DC error self-correcting circuit connects to the output node of the first LPF in Figure 2, so that Vlpf1 is the output signal of the first LPF. V_{bal} is the balance DC voltage of total circuit. V_{outadd} is the output signal of this DC error self-correcting circuit.

Since the value R4、R5、R6 and R7 are equal, we could get the following equation:

$$V_{outadd} = -(V_{lpf1} - V_{dc}) + V_{bal} \quad (23)$$

In equation (23), V_{lpf1} includes both the DC coupling signal and the desired signal. If V_{dc} equals to the DC coupling signal, then DC component of V_{outadd} equals to V_{bal}, which is also the balance voltage of total circuit. In this case, the DC coupling signal V_{err-dc} is cancelled.

By now, the key problem is how to make sure V_{dc} equals to the DC coupling signal. The integrator and LPF in Figure 9 give the solution of this problem. The two-order LPF keeps the DC component of V_{outadd}. As the integrator, the current i is integrated by capacitor C8, so that the value of V_{dc} changes until i equals to zero. If i equals to zero, that means no electrical current flows through R10, so that the voltage V_{lpfout} equals to V_1 in Figure 9. Since V_1 always equals to V_{bal} because of the character of operational amplifier, the finally stable condition of this circuit is that V_{lpfout} equals to V_{bal}. As discussed before, V_{lpfout} is the DC component of V_{outadd}, so that in stable condition, the DC component of V_{outadd} equals to V_{bal}, the DC coupling signal is cancelled.

Add the circuit shown in Figure 9 into the first LPF output node, and suppose deviation between C1 and C2 is 1% of their stable value, we could get the simulation shown in Figure 10. The signal of V_{lpf1} has a DC component equals to 11.37V, it is identical as the signal of non-ideal condition at the same node shown in Figure 8. Approximately at 0.32S, the circuit comes to the stable condition. It is shown in Figure 10 that in the stable condition, the voltage value of

V_{dc} is 11.37V, equals to the DC component of signal V_{lpf1}. And the voltage value of signal V_{lpfout} is 9V, equals to the balance voltage of circuit system.

Figure 11 is the detail of signal Voutadd and signal V_{lpf1}. It can be observed that the DC coupling signal has already been cancelled. Meanwhile, the amplifier offset voltage could also be eliminated by this circuit.

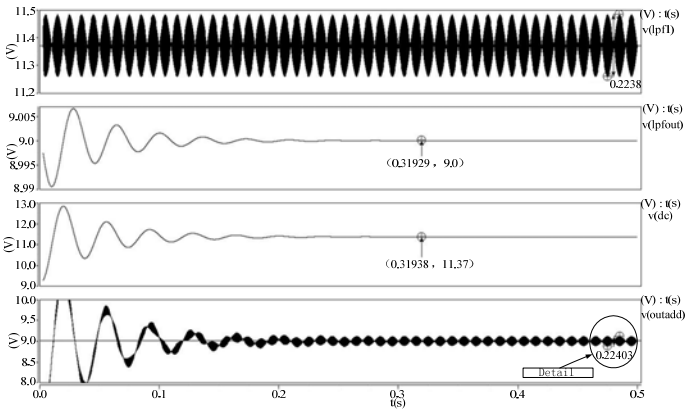

Figure 10. Simulation results of DC error self-correcting circuit

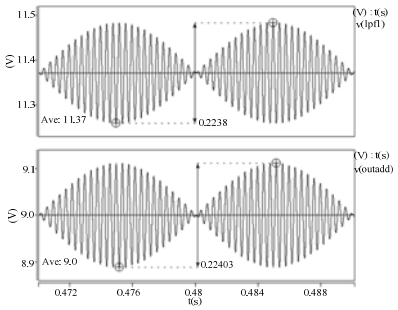

Figure 11. Details of Simulation results of DC error self-correcting circuit

Figure 12 is the picture of test board of micromachined gyroscope system. This system is used to validate the function of DC error self-correcting circuit. Inside the metal shell, there is a gyroscope sensor and the integrated circuit chip. The total integrated circuit consists of the inside chip and electrical circuit on the PCB. The power supply voltage is single 18V, so that the balance voltage of the system is 9V.

Figure 13 is the testing results of test board shown in Figure 12, in which channel one (ch1 for short in Figure 12) is the signal at the output node of the first LPF, its average is 11.5V, so that the DC component of this signal is 11.5V. This value has a departure compared to the system balance voltage 9V. It is caused by the deviation between two sensing capacitors. In Figure 12, channel two (ch2 for short in Figure 12) is the signal at the output node of the DC error self-correcting circuit. The average of this signal is almost 9V, identical to the system balance voltage. From the testing results, it could conclude that the DC error self-correcting circuit works properly.

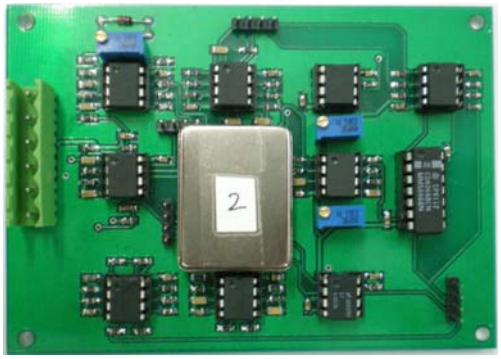

Figure 12. Picture of test board of micromachined gyroscope system

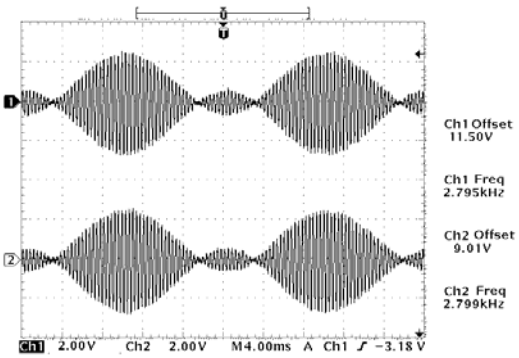

Figure 13. Measurement of input signal and output signal of DC error self-correcting circuit

6. Conclusion

The variations of driving capacitor and sensing capacitor are analyzed based on the principle of integrated circuit. It is shown that the effect caused by driving capacitor variation would be cancelled in the signal processing, but the driving capacitor variation would cause a DC error signal at the output node of the first LPF in the integrated circuit. This DC error would distort the desired signal at the output node of the amplitude amplifier. So that a DC error self-correcting circuit is designed, both the simulation results and the testing results show that DC error could be self-corrected by this additional circuit.

Acknowledgements

This work was supported by the "National Natural Science Foundation of China"(No. 61204122), the "Science and Technology Project of Xiamen"(No. 3502Z20123034), and the "Science and Technology Project of Quanzhou" (No. 2012Z98).

References

[1] Geen JA. *Very Low Cost Gyroscopes*. In Proceedings of IEEE Sensors. Irvine, USA. 2005; 1: 537-540.
[2] Neul R, Gomez U, Kehr K, Bauer W, Classen J, Doring C, Esch E, Giotz S, Hauer J, Kuhlmann B, Lang C, Veith M, Willig R. *Micromachined Gyros for Automotive Applications*. In Proceedings of IEEE Sensors. Irvine, USA. 2005; 1: 527-530.
[3] Weinberg MS, Kourepenis A. *Error Sources in In-plane Silicon Tuning-fork MEMS Gyroscopes*. *Journal of Microelectromechanical Systems*. 2006, 15(3): 479-491.
[4] Zhang Z, Hu W, Liu F, Gan W, Yang Y. *Vibration Error Research of Fiber Optic Gyroscope in Engineering Surveying. TELKOMNIKA Indonesian Journal of Electrical Engineering.* 2013; 11(4).
[5] Cai H, Ding K, Yu T. *Research on Fiber Optic Gyroscope Test Data Management System. TELKOMNIKA Indonesian Journal of Electrical Engineering.* 2013; 11(5).
[6] Gunthner S, Egretzberger M, Kugi A, Kapser K, Hartmann B, Schmid U, Seidel H. *Compensation of Parasitic Effects for a Silicon Tuning Fork Gyroscope*. *IEEE Sensors Journal*. 2006; 6(3): 596-603.
[7] Arnold E, Nuscheler F. *Compensation Methods for a Silicon Tuning Fork Gyroscope*. *Microsystem Technologies*. 2008; 14(3): 623-628.
[8] Acar C, Schofield A R, Trusov A A, Costlow L E, Shkel A M. *Environmentally robust MEMS vibratory gyroscopes for automotive applications. IEEE Sensors Journal.* 2009; 9: 1895–1906.
[9] Seidel H, Schmid U, Schwarz P, Kirsch C, Kulygin A. *Study on the lower resolution limit and the temperature-dependent performance of a surface micromachined gyroscope.* In IEEE 21st International Conference on Micro Electro Mechanical Systems. Piskataway, USA. 2008; 3: 868–871.
[10] Xie L, Wu X, Li S, Wang H, Su J, Dong P. *A z-axis quartz cross-fork micromachined gyroscope based on shear stress detection. Sensors.* 2010; 3: 1573–1588.
[11] Clark J V, Pister S J. *Modeling, simulation, and verification of an advanced micro mirror using SUGAR. Journal of Microelectromechanical Systems.* 2007; 6: 1524–1536.
[12] Xu J, Yuan W, Chang H, Lv X, Yu Y. *Hybrid macromodels for modeling and simulation of a Z-axis micro accelerometer.* In Proceedings of IEEE NEMS. Sanya, China. 2008; 2: 357–361.
[13] Hu Z, Ji C, Luo Y. *SVDbased MEMS Dynamic Testing Technology. TELKOMNIKA Indonesian Journal of Electrical Engineering*. 2013; 11 (1): 57-62.